Photosynthetic Quantum Yield Dynamics: from Photosystems to Leaves

Hogewoning, S.W.; Wientjes, I.E.; Douwstra, P.; Trouwborst, G.; van Iperen, W.; Croce, R.; Harbinson, J.

published in
The Plant Cell
2012

DOI (link to publisher)
10.1105/tpc.112.097972

document version
Publisher's PDF, also known as Version of record

This article is a *Plant Cell* Advance Online Publication. The date of its first appearance online is the official date of publication. The article has been edited and the authors have corrected proofs, but minor changes could be made before the final version is published. Posting this version online reduces the time to publication by several weeks.

Photosynthetic Quantum Yield Dynamics: From Photosystems to Leaves[W][OA]

Sander W. Hogewoning,[a,1,2] Emilie Wientjes,[b,c] Peter Douwstra,[a] Govert Trouwborst,[a] Wim van Ieperen,[a] Roberta Croce,[b,c] and Jeremy Harbinson[a]

[a] Department of Plant Sciences, Horticultural Supply Chains Group, Wageningen University, 6700 AP Wageningen, The Netherlands
[b] Department of Biophysical Chemistry, Groningen Biomolecular Sciences and Biotechnology Institute, University of Groningen, AG 9747 Groningen, The Netherlands
[c] Department of Physics and Astronomy, Faculty of Sciences, VU University Amsterdam, 1081 HV Amsterdam, The Netherlands

The mechanisms underlying the wavelength dependence of the quantum yield for CO_2 fixation (α) and its acclimation to the growth-light spectrum are quantitatively addressed, combining in vivo physiological and in vitro molecular methods. Cucumber (*Cucumis sativus*) was grown under an artificial sunlight spectrum, shade light spectrum, and blue light, and the quantum yield for photosystem I (PSI) and photosystem II (PSII) electron transport and α were simultaneously measured in vivo at 20 different wavelengths. The wavelength dependence of the photosystem excitation balance was calculated from both these in vivo data and in vitro from the photosystem composition and spectroscopic properties. Measuring wavelengths overexciting PSI produced a higher α for leaves grown under the shade light spectrum (i.e., PSI light), whereas wavelengths overexciting PSII produced a higher α for the sun and blue leaves. The shade spectrum produced the lowest PSI:PSII ratio. The photosystem excitation balance calculated from both in vivo and in vitro data was substantially similar and was shown to determine α at those wavelengths where absorption by carotenoids and nonphotosynthetic pigments is insignificant (i.e., >580 nm). We show quantitatively that leaves acclimate their photosystem composition to their growth light spectrum and how this changes the wavelength dependence of the photosystem excitation balance and quantum yield for CO_2 fixation. This also proves that combining different wavelengths can enhance quantum yields substantially.

INTRODUCTION

For well over half a century, it has been known that the energy conversion efficiency of incident photons to chemical energy by leaves is wavelength dependent (Hoover, 1937). This is due to several processes that can be divided into two classes. First, the absorption of incident irradiance by a leaf is wavelength dependent due to the different absorptance spectra of the different leaf pigments. Second, even on an absorbed light basis, different wavelengths have different quantum yields for CO_2 fixation or O_2 evolution: Red light (600 to 640 nm) has the highest quantum yield, whereas blue and green light (400 to 570 nm) are considerably less efficient in driving photosynthesis (McCree, 1972b; Inada, 1976; Evans, 1987). Maximum quantum yields for C_3 leaves were found to be close to 0.093 mol CO_2 fixed (Long et al., 1993) or 0.106 mol O_2 evolved (Björkman and Demmig, 1987) per mol absorbed photons.

Three major causes for the wavelength dependence of the quantum yield for absorbed photons have been identified (i.e., absorption by photosynthetic carotenoids, absorption by nonphotosynthetic pigments, and an imbalanced excitation of the two photosystems) (Terashima et al., 2009). Photosynthetic carotenoids have absorption maxima for blue wavelengths and differ in their efficiency (35 to 90%) for excitation energy transfer to chlorophylls, depending on the type of carotenoid and its position within the photosynthetic apparatus, whereas the energy transfer efficiency in the antenna complexes from chlorophyll to chlorophyll is 100% (Croce et al., 2001; de Weerd et al., 2003a, 2003b; Caffarri et al., 2007). Nonphotosynthetic pigments, such as flavonoids and free carotenoids, also absorb light, predominantly in the UV region but also in the blue and green part of the spectrum (e.g., anthocyanins). Nonphotosynthetic pigments do not transfer any absorbed energy to the photosynthetic apparatus. Finally, the pigment composition and absorbance properties differ for photosystem I (PSI) and photosystem II (PSII); consequently, the balance of excitation between the two photosystems is wavelength dependent (Evans, 1986, 1987; Chow et al., 1990; Melis, 1991; Walters and Horton, 1995). Any imbalance in excitation of the two photosystems results in quantum yield losses (Pfannschmidt, 2005). However, a quantitative understanding of the relative contribution of each of these factors causing quantum yield losses is still lacking.

Plants are continuously exposed to spectral changes, in the short term due to changes in weather and sun angle and in the longer term when leaves become shaded by other leaves or when shaded leaves become exposed to full sun (e.g., after canopy gap formation). The degree of shading by other vegetation strongly affects both the light intensity and spectrum to which a leaf is exposed. Spectral changes can directly alter the

[1] Current address: PlantLighting.nl, Julianaweg 78, 3525 VH Utrecht, The Netherlands.
[2] Address correspondence to sander.hogewoning@gmail.com.
The author responsible for distribution of materials integral to the findings presented in this article in accordance with the policy described in the Instructions for Authors (www.plantcell.org) is: Jeremy Harbinson (jeremy.harbinson@wur.nl).
[W]Online version contains Web-only data.
[OA]Open Access articles can be viewed online without a subscription.
www.plantcell.org/cgi/doi/10.1105/tpc.112.097972

photosynthetic quantum yield via changes in the relative absorbance by the different pigments and via changes in photosystem excitation balance. Acting on a time scale of minutes, state transitions are believed to redirect excitation energy from one photosystem to another (Haldrup et al., 2001), although in intact leaves no subsequent increase in the quantum yield for CO_2 fixation has been found (Andrews et al., 1993). In the longer term, photosynthetic organisms can adapt to spectral changes by altering the relative size of the two photosystems, thus, at least partly restoring the excitation balance between them (Chow et al., 1990; Melis et al., 1996; Fujita, 1997). In leaves, acclimation to the spectral environment resulted in an increase in the quantum yield for CO_2 fixation and linear electron transport (Walters and Horton, 1995) and an altered PSI:PSII ratio (Chow et al., 1990). However, the consequences of acclimation of the photosystem composition to the spectral environment for the wavelength dependence of the photosystem efficiency balance and how this relates quantitatively to the quantum yield for CO_2 fixation have so far not been explored.

Combined in vivo chlorophyll fluorescence and 820-nm absorbance change (ΔA_{820}) measurements (Baker et al., 2007) can be used to estimate the functional photosystem efficiency balance (Eichelmann and Laisk, 2000). The spectroscopic properties of isolated pigment-protein complexes (i.e., in vitro) can likewise be used to estimate the photosystem excitation balance (Evans and Anderson, 1987). Due to inefficiencies in excitation energy transfer and charge separation and nonlinear electron transport processes, such as cyclic electron transport, back-reactions, or transfer to O_2, the relationship between excitation balance, absorbance balance, and a more functional photosystem efficiency balance is not simple.

In this study, we explore the relationship between the wavelength dependence of the in vitro photosystem absorbance balance and the in vivo photosystem efficiency balance and how this balance relates to the quantum yield for CO_2 fixation. We also show how the growth spectrum affects the wavelength dependence of the quantum yield for CO_2 fixation in leaves. Cucumber (*Cucumis sativus*) was grown under an artificial sunlight spectrum, blue light, and an artificial shade light spectrum, the latter containing a stronger intensity at wavelengths >680 nm, thus preferentially exciting PSI. The blue growth spectrum (~445 nm) used is expected to excite the photosystems in a similar ratio as the sunlight (Evans and Anderson, 1987) but has earlier been shown to produce some distinct physiological effects (e.g., sun-type photosynthetic characteristics and a shade-type phytochrome equilibrium; Hogewoning et al., 2010c). By combining both an in vitro and in vivo approach we unambiguously show how acclimation to growth spectrum results in changes in the relative absorptance of the two photosystems, which are directly linked to changes in photosystem excitation balance and quantum yield for CO_2 fixation.

RESULTS

Quantum Yield for CO_2 Fixation

The wavelength dependence of the quantum yield for CO_2 fixation under nonphotorespiratory conditions (0.038% CO_2; 2% O_2) was measured on cucumber leaves developed under three different growth-light spectra (sunlight spectrum, shade light spectrum, and blue light; Figure 1). All measurements were performed under light-limited conditions as indicated by the fact that the assimilation-irradiance response was typically highly linear ($R^2 \geq 0.997$; see Supplemental Figure 1 online). The quantum yield for CO_2 fixation on an incident irradiance basis, which is an ecophysiologically relevant parameter, was highest in the range 620 to 680 nm in all three treatments (Figure 2A; see Supplemental Table 1 online). From 427 to 560 nm, the yield changed relatively little and was ~70% of the highest yield measured, while at 400 nm, the yield was higher than in the range 427 to 560 nm ($P < 0.05$ for sunlight and shade light spectrum, but for blue light not at all wavelengths). Above 680 nm, the yield declined rapidly down to zero at 736 nm. Differences in the absorptance spectra of the leaves from the three different growth conditions were small (Figure 3). The maximum value for the quantum yield for CO_2 fixation on an absorbed light basis (α), which is more relevant than the yield on an incident light basis with respect to our research objectives, was 0.093 CO_2 fixed per absorbed photon at 620 to 640 nm (Figure 2B; see Supplemental Table 2 online). Compared with the quantum yield for CO_2 fixation on an incident light basis, the wavelength range producing the highest values of α (580 to 640 nm) was found at shorter wavelengths (Figure 2). In the green region (520 to 580 nm) and far-red (FR) region (≥700 nm), the differences between quantum yield on an incident (Figure 2A) and absorbed (Figure 2B) light basis are greatest due to the relatively low absorptance of these wavelength ranges.

The overall wavelength response pattern of α (Figure 2B) is similar to that observed in previous studies (McCree, 1972b; Inada, 1976). However, the growth light spectrum affected α to a considerable extent. At wavelengths >680 nm, which are usually considered as PSI light, the leaves grown under a shade light spectrum produced a higher α than those grown under a sunlight spectrum or blue light (Figure 2B; $P < 0.05$ at 700 nm for the shade light spectrum versus the sunlight spectrum and the blue light, $P < 0.05$ at 710 nm for the shade light spectrum

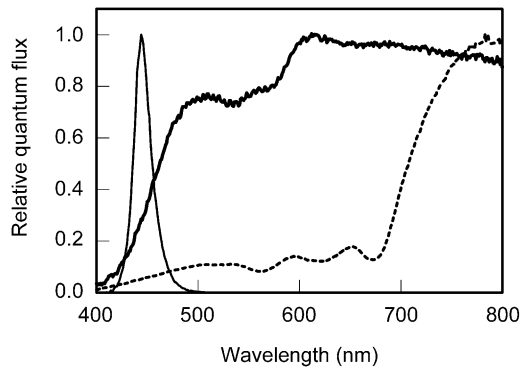

Figure 1. Growth-Light Spectra.

Spectral distribution of the artificial sunlight spectrum (thick solid line), the artificial shade light spectrum (dotted line), and blue light (thin solid line) used as growth light sources during leaf development.

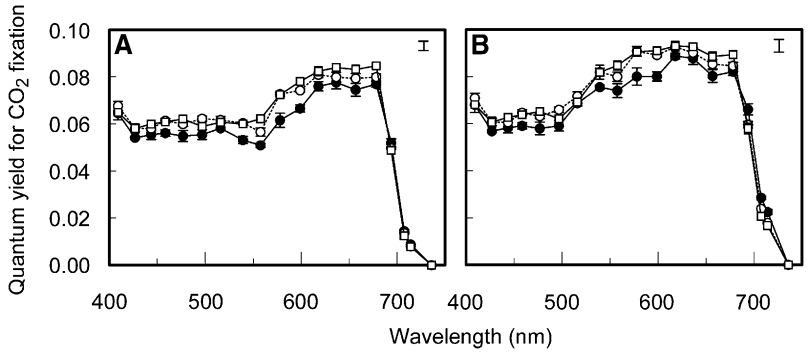

Figure 2. Wavelength Dependence of Photosynthetic Quantum Yield.

The quantum yield for CO_2 fixation for 19 different wavelengths on an incident light **(A)** and absorbed light **(B)** basis of cucumber leaves developed under a sunlight spectrum (open circles), a shade light spectrum (closed circles), and blue light (open squares). Error bars through data points represent the SE; the error bar in the top right corner represents Fisher's LSD ($P < 0.05$, $n = 3$) of the significant interaction between the means of growth light spectrum and measuring light spectrum effects.

versus blue light). Below 680 nm, which is usually considered to be PSII light, α of leaves grown under the sunlight spectrum and the blue light was higher than α of leaves grown under the shade light spectrum in the range 480 to 600 nm (except at 520 nm) and at 660 nm ($P < 0.05$ for shade light spectrum versus sunlight spectrum and/or blue light). However, <460 nm, at 520 nm and at 620 to 640 nm, α did not differ significantly for the leaves grown under the three different spectra. Across the spectrum, no significant difference between α of the sunlight spectrum and the blue light grown leaves was found.

Quantum Yield for Electron Transport through PSI and PSII

The quantum yield for CO_2 fixation was strictly light limiting for the actinic light intensity range used (see Supplemental Figure 1 online). However, the quantum yield for electron transport through PSII (Φ_{PSII}) decreased with increasing irradiance at those wavelengths where PSII was overexcited (i.e., $\Phi_{PSII} < 0.8$; Figure 4). Possibly alternative electron sinks on the PSII acceptor side played a significant role at very low irradiances (see Discussion). Therefore, it appeared most reasonable to use the Φ_{PSI} and Φ_{PSII} values associated with the highest light-limited irradiance for the calculation of the photosystem efficiency balance in vivo (see below). The efficiency of the electron transport by open PSII traps (F_v'/F_m') was consistently close to 0.8. This, together with the linear relationship between Φ_{PSII} and the PSII efficiency factor (q_p; Figure 5), implies that within the light-limited irradiance range used, the loss of Φ_{PSII} was wholly due to decreases in q_p, with no contribution from nonphotochemical quenching. While q_p indicates the fraction of photochemical quenching, q_L provides an estimate of the fraction of open PSII centers (with primary electron accepting plastoquinone of PSII [Q_A] oxidized) following the lake model for PSII (Kramer et al., 2004). The relationship of q_L with Φ_{PSII} was curvilinear (Figure 5C). The low values of q_L (i.e., <0.4) show how reduced Q_A can become even at light-limited irradiances in the case of PSII overexcitation (Figures 4A and 5C).

The wavelength dependence of Φ_{PSI} and Φ_{PSII} is shown in Figure 6A. Overall Φ_{PSI} is close to 1.0 at wavelengths <680 nm, whereas it drops progressively at ≥680 nm, which, as expected, indicates that the longer wavelengths overexcited PSI. However, a slight overexcitation of PSI was also found for the sunlight spectrum and the blue light–grown leaves at 380 to 400 nm and at 520 nm, where Φ_{PSI} was smaller ($P < 0.05$) than at 460 to 500nm at which PSII is overexcited. Maximum values for Φ_{PSII} (~0.8) were measured >680 nm for all growth light treatments and for the sunlight spectrum and the blue light grown leaves at wavelengths below 460 nm and at 520 nm. The lowest Φ_{PSII} values were measured around 480, 560, and at 660 nm, indicating significant overexcitation of PSII. Overall for the shade light spectrum–grown leaves, Φ_{PSII} was lower at wavelengths <680nm, whereas Φ_{PSI} was higher at wavelengths >680 nm, compared with the sunlight spectrum and blue light–grown leaves (Figure 6A), which is similar to the pattern found for α (Figure 2B).

Notably, besides wavelengths producing a Φ_{PSI} or Φ_{PSII} close to maximal (1.0 and 0.8, respectively), there was a range of

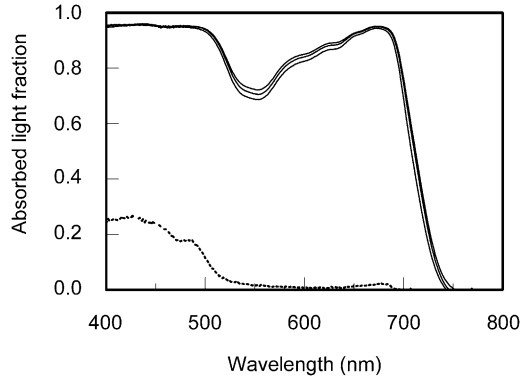

Figure 3. Leaf Absorptance Spectra.

Absorptance spectra of green cucumber leaves grown under a sunlight spectrum (middle solid line), shade light spectrum (bottom solid line), and blue light (top solid line) spectrum and the absorptance spectrum of albino cucumber leaves (dotted line).

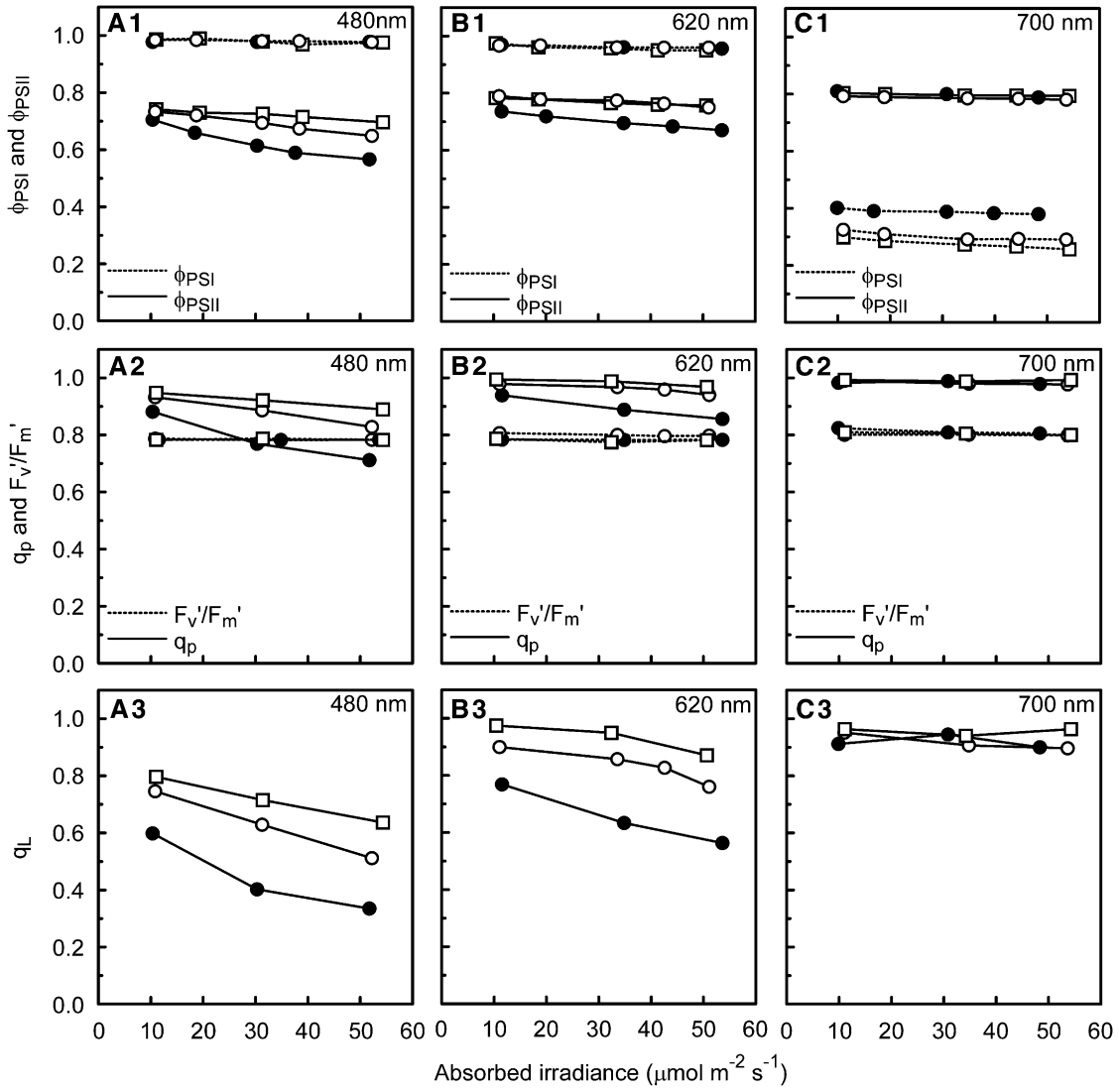

Figure 4. Responses of a Range of Photosynthetic Parameters to Irradiance Preferentially Exciting Either PSI (700 nm) or PSII (480 nm), or Exciting Both Photosystems nearly Equally (620 nm).

Response of the photosynthetic parameters Φ_{PSI} and Φ_{PSII} (top), q_p and F_v'/F_m' (middle), and q_L (bottom) for cucumber leaves grown under a sunlight spectrum (open circles), shade light spectrum (closed circles), and blue light (squares) to absorbed actinic irradiance (light-limited range) of 480 nm **(A)**, 620 nm **(B)**, and 700 nm **(C)**.

wavelengths where neither Φ_{PSI} nor Φ_{PSII} was at its maximum. At the narrow range of efficiencies associated with these wavelengths (i.e., $0.94 < \Phi_{PSI} < 0.98$), Φ_{PSI} and Φ_{PSII} changed proportionately and inversely (Figure 6A, inset). This phenomenon may be related to differences in the photosystem stoichiometry of cell layers through the leaf cross section due to the spectral changes of light penetrating into the leaf. Nevertheless, no consistent pattern of differences in Φ_{PSII} measured with red and green (deeper leaf penetration) excitation wavelengths was found. The high values of Φ_{PSII} at very low irradiances, as described above, make further analysis of these results speculative.

The measurements of Φ_{PSII} (Figure 6A) were taken after the leaf was exposed to the actinic light for sufficient time to allow for possible state transitions (≥15 min). The ratio of F_0' and F_0 can be used as an indicator for state transitions in the absence of nonphotochemical quenching (Allen, 1992; Samson and Bruce, 1995). At those wavelengths where Φ_{PSII} is well below its maximum of 0.8 and, therefore, PSII is excited more than PSI, F_0' was almost 10% lower than F_0, consistent with the development of a state transition, whereas at wavelengths overexciting PSI, F_0' and F_0 were similar (Figure 6B). Notably, the ratio of F_0' and F_0 is at its lowest value over a broader range of wavelengths in the shade light spectrum–grown leaves than in the sunlight spectrum– and blue light–grown leaves, which is consistent with the broader range of wavelengths overexciting PSII in the shade light spectrum leaves (Figure 6).

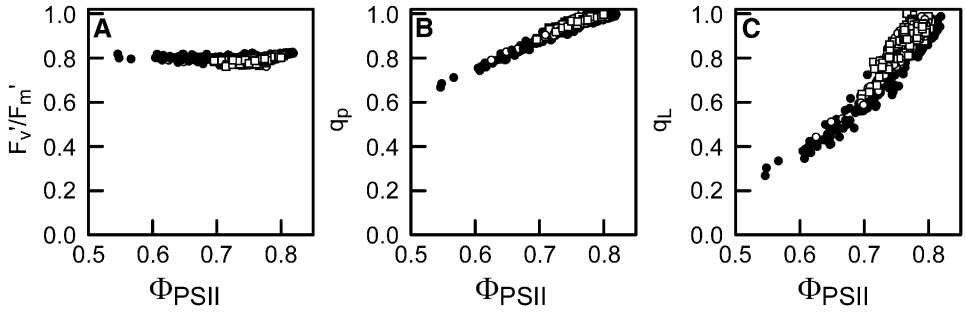

Figure 5. Relationship between F_v'/F_m', Photochemical Quenching, the Fraction of Oxidized Q_A, and the Relative Quantum Yield of PSII.

Relationship of the chlorophyll fluorescence derived parameters F_v'/F_m' **(A)**, q_p **(B)**, and q_L **(C)** with Φ_{PSII}. The data corresponding with all wavelengths of actinic light used (380 to 740 nm), and all different light intensities used per wavelength, are plotted for the three different growth light treatments (sunlight spectrum, open circles; shade light spectrum, closed circles; blue light, squares).

Photosystem Composition and Excitation Balance

To relate the in vivo parameters to the molecular composition of the photosynthetic apparatus, the pigment and protein composition of the leaves developed under the three growth light spectra was determined. The chlorophyll *a*:*b* ratio was lowest in the leaves grown under the shade light spectrum and slightly lower in the sunlight spectrum–grown leaves compared with the blue light–grown leaves (Table 1). This difference in chlorophyll *a*:*b* ratio can have two origins: (1) a change in the antenna size of PSII or (2) a change in the PSI/PSII ratio. To discriminate between these two possibilities, the protein composition of the thylakoid membranes was analyzed by SDS-PAGE and protein quantification (see Methods). The sunlight– and shade light spectrum–grown leaves showed a virtually identical PSII antenna size (Tables 1 and 2; see Supplemental Figure 2 online), while the PSI:PSII ratio was significantly lower for the shade light spectrum leaves. In the blue light–grown leaves, a slightly reduced amount of light-harvesting complex II (LHCII) was observed, while the PSI:PSII ratio was identical to that of the sunlight spectrum–grown leaves. The lower PSI:PSII ratio found for the shade light spectrum–grown leaves compared with the sunlight spectrum– and blue light–grown leaves was confirmed by protein immunoblot analysis (see Supplemental Figure 3 online). The two methods produced similar relative differences between the PSI/PSII ratios of the leaves grown under the different light spectra.

The stoichiometry between the complexes was used to scale their absorbance spectra (spectra for PSII supercomplex, PSI-light-harvesting complex I (LHCI), and LHCII in Supplemental Figure 4 online), thus allowing calculation of an estimate of the wavelength dependence of the excitation balance of the two photosystems. A comparison of this in vitro photosystem excitation balance with the in vivo photosystem efficiency balance (i.e., derived from Φ_{PSI} and Φ_{PSII} at the highest actinic light intensity used at each wavelength) revealed a strong linear relationship (Figure 7). Note that the linearity (Figure 7B) is improved if the data corresponding with the wavelengths 460 and 500 nm, which are dominated by carotenoid absorption, are not taken into account (see Supplemental Figure 5 online). Excitation in vitro at those wavelengths overexciting PSII (i.e., PSII light) appears to be more imbalanced than in vivo, where state transitions play a role. For PSI light, the two approaches produce similar results. The apparently stronger overexcitation of PSII in vitro is illustrated by the different slopes of the relationship between the two approaches for the data points corresponding with PSI light and PSII light (Figure 7B).

The Impact of Photosystem Excitation Balances on the Quantum Yield for CO_2 Fixation: Significance of Enhancement Effects

The photosystem efficiency balances in vivo (Figure 7A) were used to estimate a corresponding wavelength dependency of the quantum yield for CO_2 fixation (i.e., α_{est}; see Methods). In this calculation, quantum yield losses attributable to light absorption by photosynthetic carotenoids and nonphotosynthetic pigments are not taken into account. The values of the in vivo α calculated from gas exchange measurements (as in Figure 2B) were similar to the values of α_{est} at wavelengths $\geq$580 nm (Figure 8), except at 700 nm and at 680 nm (shade light spectrum–grown leaves). However, while the photosystem efficiency balance apparently determined the wavelength dependency of α at wavelengths $\geq$580 nm, it did not at wavelengths $\leq$560nm where photosynthetic carotenoids and nonphotosynthetic pigments absorb. At these shorter wavelengths, α_{est} overestimated α considerably (up to 50% in the range 420 to 460 nm). The absorptance spectrum of the albino leaves, which had a visually white appearance and were largely free of chlorophyll and carotenoids, is shown as a qualitative illustration of an absorptance spectrum by nonphotosynthetic leaf pigments (Figure 3). The albino leaves absorbed substantially at wavelengths <520 nm, whereas at longer wavelengths, absorptance was close to zero.

At the red wavelengths (620 to 640 nm) that produced the highest values of α (i.e., 0.093 for the sunlight spectrum and blue light, and 0.088 for the shade light spectrum–grown leaves; Figure 2B), PSII was also overexcited. This overexcitation was minor for the sunlight spectrum– and blue light–grown leaves (Φ_{PSII} = 0.76 and 0.74, respectively) but more considerable for the shade light spectrum leaves (Φ_{PSII} = 0.67; Figure 6A). A correction for the fraction of quantum yield loss due to these photosystem efficiency imbalances (see Methods) resulted in a calculated mean maximum quantum yield for CO_2 fixation of

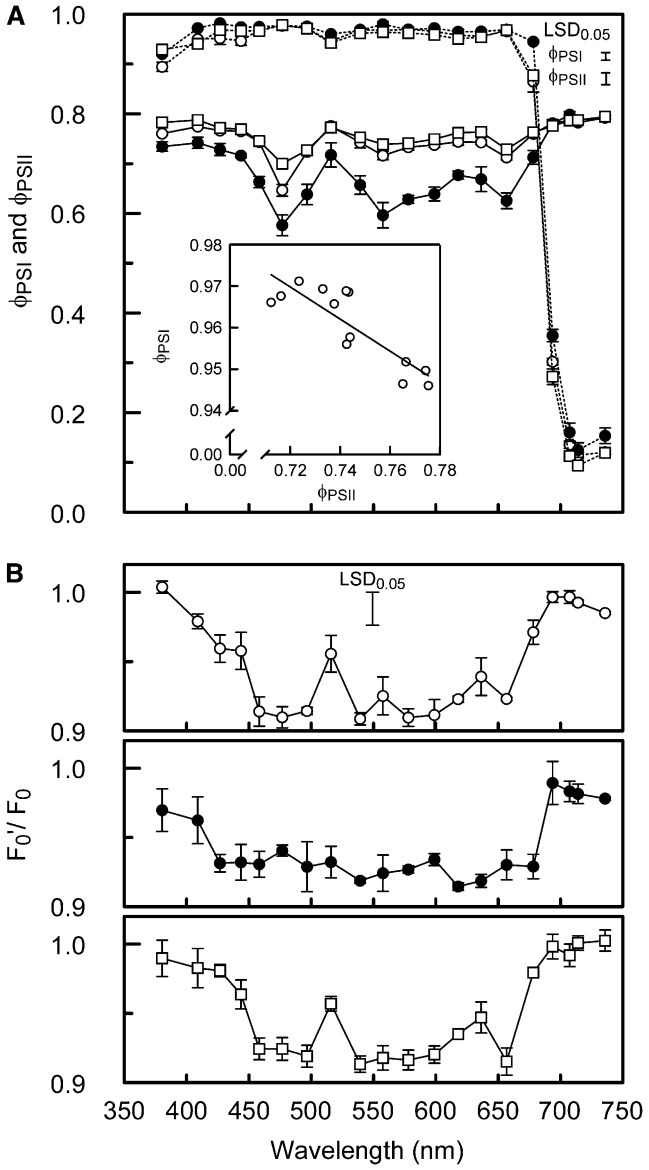

Figure 6. Wavelength Dependence of Φ_{PSI}, Φ_{PSII}, and the Development of State Transitions.

(A) Wavelength dependence of Φ_{PSI} (dashed lines) and Φ_{PSII} (solid lines) of leaves exposed to an irradiance just below an intensity high enough to be no longer light-limited (in the range 50 to 55 μmol m^{-2} s^{-1} for most wavelengths). The open circles, closed circles, and squares correspond to sunlight spectrum–, shade light spectrum–, and blue light–grown cucumber leaves, respectively. The inset shows the relationship between Φ_{PSI} and Φ_{PSII} found for sunlight spectrum leaves for the wavelengths that produced values of Φ_{PSI} within the efficiency range of 0.94 to 0.98.
(B) Wavelength dependence of the ratio of light-adapted minimum fluorescence (F_0') and dark-adapted minimum fluorescence (F_0), as an indicator of state transitions induced by the actinic measuring light ($F_0'/F_0 = 1$ indicates state 1; symbols are as in **(A)**.
Error bars through data points represent the SE; the error bars in the top right corner in **(A)** and top middle in **(B)** represent Fisher's LSD ($P < 0.05$, $n = 3$) of the significant interaction between the means of growth light spectrum and measuring light spectrum effects.

0.0955 ± 0.0004 for all three growth light treatments. This maximum quantum yield would apply in the case of perfectly balanced photosystem efficiency.

Additional evidence that the photosystem efficiency balance has a strong impact on α is provided by the gas-exchange measurements under broadband light. The quantum yield of both the shade light– and sunlight spectrum–grown leaves was determined for a broadband actinic light spectrum similar to the growth light spectrum over the spectral range 400 to 725nm. The quantum yields were also calculated as the weighted sum of the individual values determined for α at 19 different wavelengths (Figure 2) across the broadband actinic light spectra. For the shade light and sunlight spectrum, α was 21 and 10% higher than the weighted sum of α, respectively (Table 3). The larger enhancement effect found under the shade light spectrum is consistent with the stronger imbalances in photosystem efficiency found at all wavelengths <680 nm for the shade light–grown leaves (Figures 6A and 7).

DISCUSSION

Origin of the Wavelength Dependence of Quantum Yield

This study aims to clarify the underlying causes of the wavelength dependence of the quantum yield for CO_2 fixation and its adaptation capacity to the light spectrum of the growth environment. Previously, the wavelength dependence of photosynthetic quantum yield has been shown qualitatively (McCree, 1972b; Inada, 1976) and, at less wavelengths, also quantitatively (Evans, 1987). We found an overall similar pattern of wavelength dependence of quantum yield on both an incident and absorbed light basis (Figure 2). In contrast with earlier work, our parallel measurements of quantum yields for PSI and PSII electron transport and photosystem stoichiometry allow further analysis of the causes of this wavelength dependence of quantum yield for CO_2 fixation on an absorbed light basis (α).

Within the light-limited irradiance range, which was the case for our measurements (see Supplemental Figure 1 online), Φ_{PSI} and Φ_{PSII} are expected to be independent of irradiance in the absence of any alternative electron sinks for reducing power from PSII or back-reactions between electron acceptors and donors, even in case of an imbalanced photosystem excitation. However, even at wavelengths strongly overexciting PSII (e.g., 480 nm; Figure 6A), Φ_{PSII} was relatively high at very low irradiances (i.e., ~10 μmol^{-2} s^{-1}) and decreased with increasing irradiance (Figure 4A1). This phenomenon suggests that an alternative electron acceptor, such as O_2 (Pospísil, 2009) or possibly back-reactions (Quigg et al., 2006), are maintaining the Q_A pool in a relatively oxidized state at low irradiances, despite the insufficiency of electron transport through PSI. Notably, a reduced Q_A pool is also readily oxidized when actinic light is turned off. Though these alternative routes for oxidation of the Q_A pool increase Φ_{PSII} at low irradiances, they do not increase CO_2 fixation, so they do not appear to result in higher rates of linear electron transport. Whatever the underlying cause, these results show that the linkage between PSII electron transport

Table 1. Effect of Growth-Light Spectrum on Photosystem Composition

Growth Light	Sun	Shade	Blue
Chlorophyll *a*:*b*	2.98[b]	2.67[c]	3.10[a]
LHCII per PSII core	3.61[ab]	3.72[a]	3.29[b]
RC ratio PSI/PSII	0.90[a]	0.64[b]	0.90[a]
RC ratio PSII/(PSII+PSI)	0.53[b]	0.61[a]	0.53[b]

Chlorophyll *a*:*b* ratio, number of LHCII trimers per PSII core, and reaction center ratio of the two photosystems (expressed in two different ways) of cucumber leaves grown under the sunlight spectrum (Sun), the shade light spectrum (Shade), and blue irradiance (Blue). Different letters indicate significant differences between means ($P \leq 0.05$; $n = 3$).

and metabolism associated with CO_2 fixation is flexible under low irradiance.

The low values found for q_p and q_L (Figures 4A and 5) indicate that even at light-limited irradiance, Q_A reduction may significantly affect redox signaling (Bräutigam et al., 2009), and PSII may be vulnerable to photodamage (Yamamoto et al., 2008). The independence of Φ_{PSII} on F_v'/F_m' (Figure 5) implies that no nonphotochemical quenching developed under these strictly light-limiting conditions. As Φ_{PSII} is equivalent to the product of q_p and F_v'/F_m' (Genty et al., 1989), this lack of dependency implies that Φ_{PSII} should be determined solely by changes in q_p. The curvilinear relationship between q_L and Φ_{PSII} is expected because the lake model of PSII organization allows excitation that encounters a closed PSII trap (i.e., Q_A^-) in one photosynthetic unit to migrate to another where it can successfully produce charge separation and electron transport (Kramer et al., 2004 and references therein).

In the wavelength range 580 to 720 nm, the α value obtained by calculating efficiency losses due to imbalances in excitation of the two photosystems (i.e., α_{est}) generally agrees well with α calculated from gas exchange (Figure 8), indicating that the photosystem excitation balance determines the wavelength dependence of α in this spectral range. From 400 to 460 nm and at 520 nm, the photosystem excitation is balanced for the leaves grown under the sunlight spectrum and blue light (or nearly so; Figure 6A), but α_{est} is up to 50% higher than α (Figure 8). Energy losses at wavelengths <580 nm are to be expected due to the presence of carotenoids and nonphotosynthetic pigments in the leaf (Terashima et al., 2009). The energy transfer efficiency from carotenoids to chlorophylls in vivo has not yet been fully elucidated. However, for PSI carotenoids, a transfer efficiency of 70% has been reported for the core (de Weerd et al., 2003b) and for the light-harvesting complex (Wientjes et al., 2011). For PSII, β-carotene associated with the core has been shown to transfer energy with an efficiency of only 35% (de Weerd et al., 2003a). An energy transfer efficiency of 85 to 90% has been reported for lutein and neoxanthin in the antenna complexes of PSII (Croce et al., 2001; Caffarri et al., 2007), while violaxanthin in the loosely bound peripheral site of LHCII was shown not to transfer energy to chlorophylls (Caffarri et al., 2001). Considering that a significant fraction of the shorter wavelengths is absorbed by chlorophylls (Gitelson et al., 2002), that carotenoids still have an average energy transfer efficiency of ~65%, and that for the blue wavelengths α_{est} is up to 50% higher than α (Figure 8), a considerable proportion of the quantum yield losses at the shorter wavelengths must be attributable to nonphotosynthetic pigments. The absorptance spectrum of the albino cucumber leaves (Figure 3) was similar to that found for albino leaf zones of *Arabidopsis thaliana* in which a gene encoding a key enzyme in carotenoid synthesis was knocked out by virus-induced gene silencing (Zheng et al., 2010). These absorptance spectra qualitatively indicate that nonphotosynthetic pigments absorbed at wavelengths <520 nm, which is in agreement with the lower values of α than those of α_{est} (Figure 8). However, the albino absorptance spectra are unsuitable for quantitative analysis as the nonphotosynthetic pigment composition may be different for the albino and the green cucumber leaves (Solfanelli et al., 2006). UV and blue light are reported to stimulate the transcription of flavonoid synthesis genes in order to protect plants against photodamage (Kubasek et al., 1992; Jackson and Jenkins, 1995). However, no notable difference between α of the sunlight spectrum– and the blue light–grown leaves was found (Figure 2B), suggesting that in these leaves the synthesis of flavonoids that absorb visible light was either insensitive to blue irradiance or it was saturated by the blue light content of the sunlight spectrum.

Table 2. Chlorophyll Content Values of Different Photosystem Components

Photosystem Component	Chlorophyll No.	Chlorophyll *a*:*b*	Chlorophyll *a*	Chlorophyll *b*
PSI-LHCI	168	8.5	150.3	17.7
PSII core	37	∞	37	n.a.
LHCII trimer	42	1.3	23.7	18.3
Minor Lhcb	27	1.7	17	10

The chlorophyll content values of PSI-LHCI, PSII core, LHCII trimer, and minor Lhcb (sum of CP29, CP26, and CP24) that were used to calculate the PSI:PSII ratio from the chlorophyll *a*:*b* ratio of the membranes. For the calculation, a 1:1 ratio for PSII core:minor Lhcbs was used, while the LHCII:PSII core ratio was obtained for each sample from the analysis of the SDS-PAGE gel. The PSII core binds no chlorophyll *b*, hence the infinity sign (∞). n.a., not applicable.

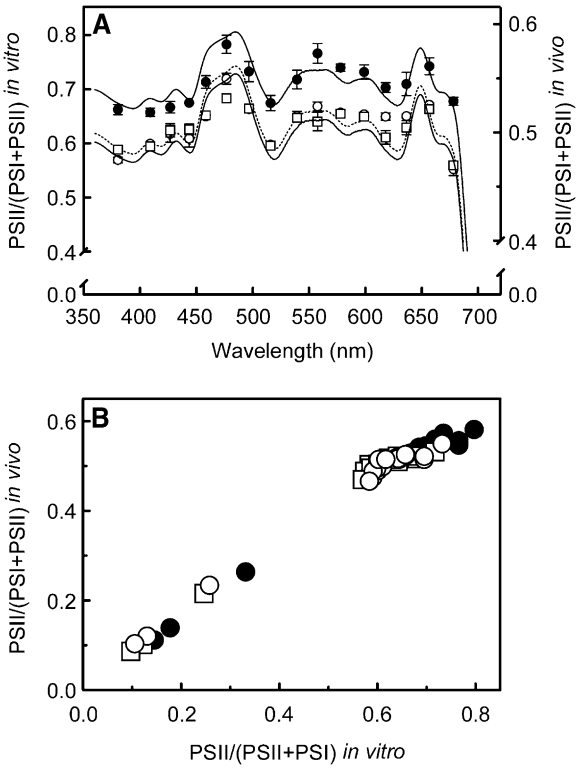

Figure 7. Wavelength Dependence of the Excitation Balance between PSI and PSII.

(A) Wavelength dependence of the excitation balance of the two photosystems calculated as absorption by PSII divided by absorption of both PSI and PSII using an in vitro (connected lines) and in vivo (unconnected data points) approach. The left *y* axis corresponds to the in vitro approach (sunlight spectrum, dashed line; shade light spectrum, top solid line; blue light, bottom solid line) and the right *y* axis with the in vivo approach (sunlight spectrum, open circles; shade light spectrum, closed circles; blue light, squares). Note that the scale is different for the two *y* axes.

(B) Relationship between the excitation balances obtained via the in vitro and in vivo approach. The data in the top right corner, which are the data in plot **(A)**, are presented in more detail in Supplemental Figure 5 online. Note that for values of PSII/(PSII+PSI) < 0.4, which correspond with wavelengths preferentially exciting PSI, both the in vitro and in vivo methods produce similar results. At values of PSII/(PSII+PSI) > 0.5, which correspond with wavelengths preferentially exciting PSII, the overexcitation of PSII appears to be stronger in vitro.

Quantum Yield and Photosystem Stoichiometry Acclimation to Growth Spectrum

At those wavelengths where the shade light spectrum–grown leaves had a lower α than the sunlight spectrum– or the blue light–grown leaves (Figure 2B), Φ_{PSII} was also lower for the shade light spectrum–grown leaves (Figure 6A). By contrast, where shade light spectrum–grown leaves had a higher α (>680 nm), their Φ_{PSI} was also higher. Therefore, the shade light spectrum leaves, grown under a spectrum with a large proportion of wavelengths overexciting PSI (Figure 1), use PSI light more efficiently than sunlight spectrum– and the blue light–grown leaves, whereas sunlight spectrum and the blue light leaves use PSII light more efficiently than shade light spectrum–grown leaves. The differences in the wavelength dependence of α, Φ_{PSI}, and Φ_{PSII} between the shade light spectrum leaves on the one hand and the sunlight spectrum and blue light leaves on the other are consistent with the relatively greater number of PSII reaction centers found in the shade light spectrum leaves (Table 1; confirmed by Supplemental Figure 3 online). However, the antenna size of PSII did not differ for sunlight and shade light spectrum leaves. These results are in line with those of Chow et al. (1990). It is important to distinguish the differences between sunlight and shade light in terms of spectral composition and irradiance intensity. In contrast with a shade light spectrum versus a sunlight spectrum, the antenna size of PSII is generally larger for leaves acclimated to low irradiance compared with high irradiance leaves (Walters and Horton, 1994; Bailey et al., 2001; Ballottari et al., 2007). We further show that across the spectrum of wavelengths ≤680 nm used, the excitation of PSII is higher than that of PSI in the shade light spectrum leaves, compared with the sunlight spectrum and blue light leaves, whether this is derived from in vitro or in vivo measurements (Figure 7A). This shift to increased PSII excitation dependent upon the growth spectrum clearly shows the extent and consequences of photosystem acclimation to growth light spectra exciting PSI and PSII in different proportions.

Despite the possible discrepancies between photosystem excitation balance in vitro, where only the relative absorbance of the photosystems is taken into account, and the photosystem efficiency balance in vivo, where inefficiencies in excitation energy transfer and charge separation, and cyclic electron transport, back-reactions, or transfer to O_2 can play a role, the relationship between the two approaches is highly linear (Figure 7B). This indicates that the impact of these in vivo processes at the highest light-limited actinic irradiances used was small enough to allow the measures of Φ_{PSII} and Φ_{PSI} to be used to estimate a functional excitation balance. The moderate outliers in the relationship between the two approaches (460 and 500 nm; see Supplemental Figure 5 online) are likely due to the strong absorption of these wavelengths by carotenoids, which are associated more with PSII than PSI and which on average have a lower excitation energy transfer yield when associated with PSII than PSI (see section above).

In absolute terms, the overexcitation of PSII was found to be greater in vitro than in vivo (Figure 7). This may have several origins: (1) The in vitro approach using absorbance does not incorporate a correction for losses of excitation transfer efficiency and thus overestimates the relative excitation of PSII at wavelengths where carotenoids absorb. (2) In vivo overexcitation of PSII may have been slightly underestimated due to the bias of the 640-nm measuring light used to determine Φ_{PSII} toward the adaxial leaf layers, whereas in vitro proteins from the whole leaf were measured. (3) State transitions did not play a role in vitro, whereas during the in vivo measurements state transitions partly rebalanced photosystem excitation. Any F_0' quenching accounted for by nonphotochemical quenching (Oxborough and Baker, 1997) can be ruled out in our measurements (Figure 5A). Therefore, the lower F_0' found for PSII light than for PSI light, which produced an F_0' equal to dark-adapted F_0, and the broader wavelength range producing

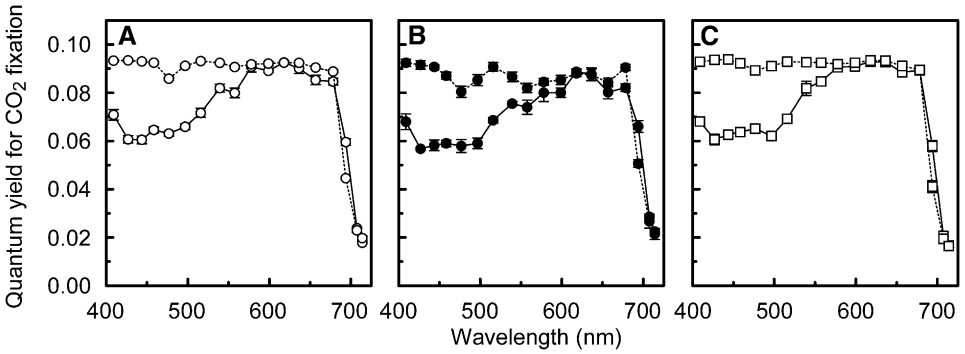

Figure 8. Wavelength Dependence of Quantum Yield Losses due to Absorption by Carotenoids and Nonphotosynthetic Pigments.

Quantum yield for CO_2 fixation for 18 different wavelengths (400 to 720 nm) calculated from gas-exchange measurements (i.e., measured values of α as in Figure 2B; solid lines) and from the in vivo efficiency balance between the two photosystems as shown in Figure 7A (α_{est}; dotted lines). Note that light absorption by carotenoids and nonphotosynthetic pigments has not been taken into account in the calculation of α_{est}. Graphs **(A)**, **(B)**, and **(C)** correspond to leaves grown under the sunlight spectrum, the shade light spectrum, and the blue irradiance, respectively. Error bars indicate the SE (n = 3).

minimal ratios of F_0' and F_0 for the shade spectrum leaves (Figure 6B), support the proposition that state transitions diminished the overexcitation of PSII in vivo. Our data also show that in the case of strong imbalances in photosystem excitation, state transitions are not capable of fully rebalancing excitation, as in vivo the PSII acceptor side is still reduced substantially over a broad range of wavelengths (Figures 6A and 7).

Despite blue light being widely used to excite PSII, it is the longer blue wavelengths (460 to 500 nm) that strongly overexcite PSII and not the blue wavelengths around 445 nm used here (Evans and Anderson, 1987; Figures 6A and 7A). However, pure blue light around 445 nm is expected to excite cryptochromes more strongly than the sunlight- and shade light spectrum in our treatments (Ahmad et al., 2002) and produces a phytochrome signaling that is closer to that of the shade light spectrum treatment than of the sunlight spectrum treatment (Sager et al., 1988; Hogewoning et al., 2010c). So far little is known on the role that nonphotosynthetic photoreceptor signaling plays in photosynthetic acclimation (Dietzel et al., 2008). Studies with photoreceptor-deficient mutants suggested that the acclimation of photosystem stoichiometry does not depend on the presence of phytochromes or cryptochromes (Walters et al., 1999; Fey et al., 2005). The lack of any significant physiological differences found between our sunlight spectrum– and blue light–grown leaves (Figures 2, 6A, and 7A) confirm this suggestion, although the amount of LHCII per PSII core was slightly lower in the blue light–grown leaves (Table 1). At least the physiological consequences for the acclimation of quantum yield to the growth spectrum are shown to be fully dependent on changes in photosystem stoichiometry and subsequent effects on photosystem efficiency balance under our experimental conditions.

The Maximum Quantum Yield for CO_2 Fixation and the Importance of Enhancement Effects

The absolute maximum quantum yield for CO_2 fixation or O_2 evolution has been a subject of debate for a long time (Govindjee, 1999). We found a maximum quantum yield of 0.093 CO_2 fixed per absorbed photon for the sunlight spectrum– and blue light grown–leaves at 620 to 640 nm (Figure 2B; see Supplemental Table 2 online). Correction for quantum yield losses due to imbalances in photosystem excitation at these red wavelengths increased the maximum value of α to 0.0955 for all three growth light treatments. Since McCree (1972a) concluded that enhancement effects are insignificantly small for white light, not much attention has been given to the issue of enhancement effects (i.e., the quantum yield of a combination of wavelengths is higher than the sum of the parts) (Emerson et al., 1957). However, we show that most wavelengths in the range 400 to 670 nm overexcited PSII slightly or more strongly, dependent on the growth light treatment, while wavelengths in the range 685 to 730 nm strongly overexcited PSI (Figures 6A and 7A), as suggested in the work of Evans and Anderson (1987). Also, leaves tune their photosystem stoichiometry to the spectrum of their growth environment, resulting in increased light use efficiency

Table 3. Quantum Yield Enhancement Effect Produced by Combining Wavelengths

Light Spectrum	α Measured	α Calculated	Enhancement
Shade light spectrum	0.085 ± 0.001	0.070 ± 0.001	21%
Sunlight spectrum	0.084 ± 0.001	0.076 ± 0.001	10%

Enhancement of the quantum yield for CO_2 fixation (α) under an actinic light spectrum similar to the growth light spectrum in comparison with α calculated as the weighted sum of 19 individual wavelengths across the actinic light spectrum (α over 400 to 725 nm; ±SE).

(see section above; Chow et al., 1990). So, while the longer wavelengths (>700 nm) individually produce relatively low values of α (Figure 2B) due to PSI overexcitation (Figures 6A and 7A), there is no reason to assume that α would be suboptimal for these long wavelengths in the presence of other wavelengths that balance the photosystem excitation. Therefore, the contribution of the longer wavelengths (700 to 730 nm) to the quantum yield is expected to be significant when measuring the maximum α with a broadband light source extending to the near infrared (NIR). Our calculation showing a significant enhancement effect on the value of α for both the shade light and sunlight spectrum, and the larger enhancement for the shade light spectrum (Table 3), confirms this expectation.

Enhancement effects have consequences for quantum yield measurements. In some studies on the maximum quantum yield, a quantum sensor (sensitivity 400 to 700 nm) was used to measure the quantum flux of broadband actinic light containing wavelengths >700 nm (Björkman and Demmig, 1987; Long et al., 1993). When the wavelength range 700 to 730 nm is not taken into account, quantum yields are overestimated because the absorbed photon flux is underestimated, and, perhaps more importantly, this wavelength range is the most important for enhancement effects. Nevertheless, Long et al. (1993) reported an average maximum α of 0.093 CO_2 fixed per absorbed photon for a range of C_3 plants of diverse life form, taxa, and habitat, which is in line with our maximum. However, they measured with a quartz-iodine lamp (white light), which is enriched in the red part of the spectrum compared with sunlight (Evans, 1987), but nevertheless substantially comprises less efficient, shorter wavelengths. Therefore, the shorter wavelengths (<580 nm) would have produced an underestimate of the absolute maximum α, while ignoring the longer wavelengths (>700 nm) would have produced an overestimate of α. In fact, the varying extent to which α is lowered at the shorter wavelengths for different species (Inada, 1976) and growth environments (McCree, 1972b) makes it difficult to compare measurements of quantum yield with actinic light containing these shorter wavelengths.

If the aim is to measure quantum yield for purposes of understanding the maximum potential conversion efficiency of photosynthetic electron transport to CO_2 fixation, it should be determined using a combination of wavelengths that (1) are not absorbed by carotenoids and nonphotosynthetic pigments (i.e., $\geq$580nm) and (2) produce a balanced photosystem efficiency, which can be monitored spectroscopically in vivo (Baker et al., 2007). In other cases, it is important that the spectrum of the actinic irradiance is provided. We conclude that the maximum quantum yield for CO_2 fixation is around 0.095 and that enhancement effects are significant.

Our study shows that photosystem efficiency balance determines the wavelength dependence of leaf photosynthetic quantum yield where absorption by carotenoids and nonphotosynthetic pigments is insignificant. It would be valuable to disentangle the contributions of photosynthetic carotenoids and nonphotosynthetic pigments to quantum yield losses quantitatively. Crop yields may be improved by breeding varieties with a lower nonphotosynthetic pigment content, especially under controlled conditions (e.g., greenhouses) with lower abiotic stress levels (e.g., drought and UV radiation). State transitions only partly counteracted imbalances resulting from illumination with PSII light. Where the plant's growth light spectrum excited the two photosystems to different degrees, the PSI:PSII ratio in the thylakoids was adjusted to increase the light use efficiency for electron transport. Interestingly, it was not the PSII antenna size but the number of PSII supercomplexes that changed. The remarkable match between the in vitro and in vivo approach used to determine photosystem excitation balance proves that measurements on isolated thylakoids can be used reliably to make an estimate of the in vivo wavelength dependence of the quantum yield for CO_2 fixation.

METHODS

Plant Material and Growth Conditions

Cucumber plants (*Cucumis sativus* cv Hoffmann's Giganta) were cultivated in a climate chamber (Hogewoning et al., 2010c) under 100 $\pm$ 5 μmol m^{-2} s^{-1} irradiance (16 h photoperiod) provided by three light sources with distinct spectra (Figure 1): an artificial sunlight spectrum (Hogewoning et al., 2010b), an artificial shade light spectrum, and blue light, the latter provided by light-emitting diodes (LEDs; center wavelength 445 nm; Hogewoning et al., 2010c). The shade light spectrum is expected to excite PSI more strongly than the sunlight spectrum and the 445 nm blue light, for which a similar photosystem excitation balance is expected (Evans and Anderson, 1987). The shade light spectrum was provided by quartz-halogen lamps filtered with a tungsten-to-daylight conversion filter (Full C.T. blue; Lee Filters) with a dielectric multilayer film reflecting near-infrared wavelengths (900 to 1200 nm; Sonneveld et al., 2009) for temperature control.

Cucumber plants derived from a F3 population in which one-third of the plants developed an albino phenotype in the tissue between the veins (De Ruiter Seeds) were grown under similar conditions but using red LEDs as the growth light.

Gas Exchange

Gas exchange was measured on leaves using a lab-built two-part leaf chamber (Hogewoning et al., 2010a). A gas mix containing 380 μmol mol^{-1} CO_2, 20.8 $\pm$ 0.4 mmol mol^{-1} water, and 20 mmol mol^{-1} O_2 in N_2 was used at a flow rate sufficient for CO_2 depletion to remain below 10 μmol mol^{-1}. Leaf CO_2 and water exchange and the atmospheric pressure were measured using a LI-7000 gas analyzer (LI-COR), and CO_2 assimilation was determined according to von Caemmerer and Farquhar (1981). Leaf temperature was maintained at 25 $\pm$ 1°C by circulating temperature-conditioned water through channels in the upper and lower leaf chamber halves and was monitored from below the leaf using a noncontact temperature sensor (Micro IRt/c; Exergen). No significant leaks in the leaf chamber seal, which might have affected the gas-exchange measurements, were found.

Actinic Light

Actinic light was projected onto the leaf from above via a randomized optical fiber split into four fibers (Heinz Walz), allowing the projection of up to four different light sources onto the leaf. The light sources used were filtered 250-W quartz-halogen lamps and a blue LED of the same type as used for blue growth light. To provide narrow-band light with 19 different wavelength bands in the range 400 to 740 nm, a quartz-halogen lamp was filtered using a NIR cutoff filter in combination with different band-pass filters: 400 nm with a 40-nm full width at half maximum (FWHM; Thorlabs); 427 nm with 15-nm FWHM (Semrock); 445 nm with 25-nm FWHM (Semrock); and 460 to 740 nm with 10-nm FWHM (Thorlabs). The filters

from Semrock were used in combination with an additional NIR filter. In the UV-A region of the spectrum, actinic light was provided using three LEDs (380-nm center wavelength; H2A1-H375; Roithner Lasertechnik) coupled to three fibers that illuminated the leaf via ports in the side of the leaf chamber. Broad-band actinic light was provided by filtering a quartz-halogen lamp with a tungsten-to-daylight conversion filter (similar to the shade light spectrum treatment) and by adding an additional NIR filter to remove the longer wavelengths from the spectrum. Rotary solenoid–driven shutters were used to interrupt the actinic light, and different light intensities of the actinic light provided by the filtered quartz-halogen lamps were set using neutral density filters.

The incident actinic light intensity was measured using the photocurrent output of a photodiode (OSD15-5T; Centronic) that sampled the irradiance in the leaf chamber via a light guide. The light guide photodiode system was calibrated in situ for each wavelength using both a thermopile calibrated against a quantum sensor (LI-COR) and the spectroradiometer (USB2000; Ocean Optics), the sensors being placed in the chamber at the same level as the leaf. The fiber optic probe of the spectroradiometer was mounted in a black holder to replicate the design of the quantum sensor, where the optical window of the sensor is located in a black background. The area surrounding the optical window of the thermopile was also painted black. The two calibration methods produced identical results. The calibration with the spectroradiometer was repeated with a cucumber leaf as a background (i.e., the fiber projected through the leaf), producing results different from those obtained with a black background, consistent with the reflectance spectrum of the cucumber leaf. The calibration with a black background underestimated the irradiance a leaf receives more at those wavelengths where reflectance is greater (e.g., 1% at 520 nm, 5% at 560 nm, 1% at 620 nm, 10% at 720 nm, and 22% at 740 nm). This is due to the radiation reflected from the leaf being reflected from the chamber interior back onto the leaf surface, and this error was corrected for. We were unable to measure the irradiance of the 380 nm radiation accurately, so for this wavelength, not all data are presented. The light distribution over the leaf chamber area was measured (Hogewoning et al., 2010a) to determine the average irradiance that the leaf received.

Chlorophyll Fluorescence

Chlorophyll fluorescence was measured using red and green excitation wavelengths as measuring light. Green excitation was obtained from a 530-nm peak emission LED (Luxeon K2) filtered by a 560-nm, 10-nm FWHM band-pass filter (Thorlabs). Red excitation was obtained from a 640-nm peak emission LED (Luxeon K2) filtered by a 660-nm short-pass filter. Both sources were modulated at different frequencies of ~1000 Hz and applied simultaneously to the leaf. The measuring light was projected onto the leaf via optical fibers inserted into ports in the side of the leaf chamber. A saturating light pulse (1.2 s; 10,000 μmol m^{-2} s^{-1}) was provided by 16 LEDs (640 nm; Luxeon Rebel) mounted on a brass ring, which supported and surrounded the optical fiber for the actinic light and served as a heat sink for the LEDs. The chlorophyll fluorescence signal was detected from below the leaf by three photodiodes (GaAsP G1736; Hamamatsu) mounted on a custom-made detector board. The photodiodes were covered with 3-mm RG9 filters that only transmit wavelengths >700 nm (Schott). The signal from the photodiodes was demodulated using two lab-built demodulators, one for each of the two excitation wavelengths. Light- and dark-adapted minimum chlorophyll fluorescence (F_0' and F_0, respectively) were measured in the absence of actinic light by first closing the shutters and then applying a 1-s pulse of FR to oxidize any reduced Q_A and ensure the measurement of a real F_0 or F_0'. Short FR pulses were provided by a quartz-halogen lamp with a band-pass filter (710 nm, 10 nm FWHM; Thorlabs) coupled into an optical fiber inserted into a port in the side of the leaf chamber.

Measurements of light-adapted steady state chlorophyll fluorescence (F′), light-saturated chlorophyll fluorescence (F_m'), and F_0' (nomenclature as in van Kooten and Snel, 1990) were used to calculate the relative PSII operating efficiency (F_q'/F_m' or Φ_{PSII}), the electron transport efficiency by open PSII traps (F_v'/F_m'), the PSII efficiency factor (F_q'/F_v' or q_p), and the fraction of Q_A oxidized (i.e., open; q_L) according to Kramer et al. (2004) and Baker (2008). The parameter q_L, calculated as $(F_q'/F_v')(F_0'/F')$, is based on the lake model for the PSII photosynthetic apparatus and provides an estimate of the fraction of open PSII centers (with Q_A oxidized; Kramer et al., 2004). Dark-adapted (20 min) F_0 and F_m measurement allowed the calculation of the maximum quantum efficiency of PSII (F_v/F_m). In the results, only data obtained from measurements with red measuring light are shown, as the parameters calculated from measurements with red and green measuring light did not differ significantly.

820-nm Absorbance Changes

The measuring light for 820-nm absorbance changes (ΔA_{820}) was provided by an LED (ELD-810-525; Roithner Lasertechnik) coupled to an optical fiber, which was inserted into a port in the side of the leaf chamber. The 820-nm signal was detected by three NIR-sensitive silicon photodiodes (BPW 34 FA; Osram) mounted on the same circuit board as the photodiodes detecting chlorophyll fluorescence and demodulated using a lab-built demodulator. The signal changes produced by interrupting the actinic light and applying and removing a 10-s FR pulse were recorded. During the FR pulse, a saturating light pulse (5 ms) was applied to the leaf to ensure a complete oxidation of the P700 pool (Kingston-Smith et al., 1999), and the rapid signal changes produced were recorded using a USB oscilloscope module (500-kHz Mephisto Scope; Meilhaus). A saturating light pulse (400 ms) from the red LED array was used to accelerate complete reduction of $P700^+$ when this reduction was slow (usually at wavelengths ≥680 nm). The relative PSI operating efficiency (Φ_{PSI}) was calculated from the signal recorded during the light-adapted steady state, the fully reduced state, and the fully oxidized state of the P700 pool (Baker et al., 2007).

Measurement of Photosynthesis Parameters

Simultaneous measurements of gas exchange (2% O_2), chlorophyll fluorescence and ΔA_{820} were made at 20 different wavelengths of actinic light in the range 380 to 740 nm on mature second leaves of intact plants with a homogeneously distributed $F_v/F_m \geq 0.8$ (verified by chlorophyll fluorescence imaging as in Hogewoning and Harbinson, 2007). Measurements were made at five light-limited irradiances, typically within the range 10 to 55 μmol m^{-2} s^{-1} absorbed irradiance, using the minimum irradiance to prevent the Kok effect (Sharp et al., 1984). The quantum yield for CO_2 fixation (α) was calculated as the slope of the linear regression between net assimilation and irradiance. When gas exchange was in steady state, steady state fluorescence (F′), the maximum fluorescence (F_m'), and ΔA_{820} were recorded at each irradiance. The light-adapted minimum fluorescence (F_0') was recorded at three irradiances per wavelength. Dark-adapted F_v/F_m was measured at the start and end of each day.

Before subjecting the leaf to a different wavelength, it was exposed to an actinic light spectrum similar to the growth light spectrum until gas exchange stabilized to prevent possible adaptation effects during measurement. At the start, middle, and end of each day, gas exchange, chlorophyll fluorescence and ΔA_{820} were measured using an actinic light spectrum similar to the growth spectrum to identify any changes in the leaf response arising during the day. Measurements taken on three plants over 3 d were required for the full sequence of 20 wavelengths. The quantum yield of the actinic light spectrum similar to the growth spectrum was determined for the irradiance absorbed between 400 and 725 nm. The slight differences between the α values for these broadband spectra that were occasionally found between the three leaves required for measurement of the full sequence of the 20 narrow-band wavelengths never

exceeded 6%. Any deviation of the average α value of these three leaves was used as a correction factor for the α values for the narrow-band wavelengths measured on the corresponding leaf. Per growth light treatment, all 20 narrow-band wavelengths were measured three times (n = 3).

Leaf Absorptance of actinic light

The absorptance spectrum of each leaf was calculated in nanometer steps from reflectance and transmittance measurements (Hogewoning et al., 2010b) made after measuring the leaf photosynthesis parameters. The absorbed light fraction was calculated for each wavelength by multiplying the absorptance spectrum with the actinic light spectrum. The effect of blue light–induced chloroplast movements (Jarillo et al., 2001) on absorptance was checked by comparing the absorptance spectrum of a dark-adapted leaf with that of a leaf exposed for 1 h to 300 μmol m^{-2} s^{-1} blue LED light (463-nm center wavelength). The difference was negligible across the spectrum ($\leq$1%). To obtain a qualitative indication of absorptance by nonphotosynthetic pigments, absorptance spectra were also measured on the albino leaves (n = 10).

Calculation of Enhancement Effect under Broadband Light

Broadband light enhancement effects on α were verified for both the shade light– and sunlight spectrum–grown leaves. For this, the quantum yield of the actinic light spectrum similar to the growth spectrum in the range 400 to 725 nm (see above) was also calculated as the weighted sum of the α values corresponding with all narrow-band wavelengths measured. First, the α value was determined in 1-nm steps in the range 400 to 725 nm by interpolation of the α value for the 19 wavelengths measured within this spectral range. The resulting column of α values was multiplied with a column containing the absorbed irradiance spectrum in 1-nm steps for each corresponding leaf. The sum of these products represents the α value for broadband light as the weighted sum of the individual wavelengths across the actinic light spectrum.

Quantification of Photosystem Composition

Thylakoids were prepared from snap-frozen leaves (Bassi et al., 1988), and the number of LHCII complexes per PSII core was evaluated by SDS-PAGE (14.5% Tris-Tricine; Schägger, 2006) and colorimetric detection. After Coomassie Brilliant Blue staining, gels were digitized with a Fujifilm LAS 300 scanner, and the optical density integrated on the area of the band was quantified using the GEL-PRO Analyzer (Media Cybernetics). The total optical density of the Lhcb1,2 and Lhcb3 band was compared with that of CP29 (the bands were identified by protein immunoblotting). To quantify the different binding of Coomassie Brilliant Blue to these polypeptides, a subcomplex containing LHCII and CP29 in a 1:1 ratio (B4; Caffarri et al., 2009) was analyzed in the same gel system. A 1.1 times stronger binding to CP29 than to LHCII was found. CP29 is assumed to be present at stoichiometric amounts with the PSII core, based on its presence in the smallest C_2S_2 (dimeric core with two strongly bound LHCII trimers) PSII supercomplex (Morosinotto et al., 2006; Caffarri et al., 2009). To our knowledge, no substantial amount of PSII core without associated Lhcb antenna can be present in wild-type plants. Eight repetitions from three different leaves per growth light treatment were used.

The PSI:PSII ratio was calculated from the measured chlorophyll *a*:*b* ratio as described by Croce et al. (2002) using the pigment-protein stoichiometry of the individual complexes (Table 2) and the number of LHCII complexes per core. A stoichiometry of 1:1 between the core and the minor antennae (CP24, CP26, and CP29) was used (Yakushevska et al., 2001). Due to the large difference in chlorophyll *a*:*b* ratio for PSI (8.5) and PSII (1.85 based on 3.6 LHCII/PSII core), this allows for an accurate estimation of the PSI:PSII ratio (for further details on the calculation, see legend of Supplemental Figure 2 online). This method was used previously to estimate the number of LHCII trimers per PSII core in PSII membranes (Broess et al., 2008). Additionally, the PSI:PSII ratio was determined by protein immunoblotting (see Supplemental Figure 3 online).

Photosystem Excitation Balance in Vivo and in Vitro

The in vivo loss of quantum yield for CO_2 fixation on an absorbed light basis that can be attributed to an imbalanced photosystem excitation was calculated for each wavelength. First, the in vivo photosystem efficiency balance was determined for each wavelength using the following equation:

$$\text{Photosystem efficiency balance} = \frac{\Phi_{PSII(max)}/\Phi_{PSII}}{\Phi_{PSI(max)}/\Phi_{PSI} + \Phi_{PSII(max)}/\Phi_{PSII}}$$

where Φ_{PSI} and Φ_{PSII} are the values measured at the highest light-limited irradiance for each wavelength. $\Phi_{PSI(max)}$ and $\Phi_{PSII(max)}$ are the values of Φ_{PSI} and Φ_{PSII} obtained under steady state excitation at those wavelengths producing a maximum efficiency for the respective photosystems (i.e., ~0.99 and 0.80 for Φ_{PSI} and Φ_{PSII}, respectively). Using these maximum efficiency values, the normalized values of Φ_{PSI} (i.e., $\Phi_{PSI}/\Phi_{PSI(max)}$) and Φ_{PSII} (i.e., $\Phi_{PSII}/\Phi_{PSII(max)}$) can be determined. We assume that under strictly light-limiting conditions, a normalized Φ_{PSI} or Φ_{PSII} that is less than the maximum limiting value is due to the overexcitation of that photosystem relative to the other. The reciprocal of the normalized efficiency is therefore a measure of the relative excitation of PSI and PSII at that actinic wavelength. The photosystem efficiency balance, which is the relative excitation balance of PSII and PSI derived from the measured photochemical yields of PSII and PSI, can then be calculated as shown in the equation above.

Second, the loss of quantum yield that can be attributed to unbalanced photosystem excitation was determined for each wavelength using the following equation:

$$\text{Fraction of quantum yield loss} = |2 * (\text{photosystem efficiency balance} - 0.5)|$$

where 0.5 represents a perfectly balanced photosystem excitation; any deviations of this value will result in a loss of yield, which is double this absolute numerical value. Subsequently, the quantum yield for CO_2 fixation was calculated from this fraction of quantum yield loss at each wavelength using the following equation:

$$\alpha_{est} = (1 - \text{fraction of quantum yield loss}) \times \alpha_{max}$$

where α_{est} represents the calculated quantum yield for CO_2 fixation that takes no account of quantum yield losses due to absorptance by photosynthetic carotenoids or nonphotosynthetic pigments (α_{max} represents the highest measured α value determined by gas exchange at 620 or 640 nm).

The wavelength dependence of the in vitro excitation balance of the two photosystems was determined using the absorbance spectra of the different photosystem components. First, LHCII and PSI-LHCI were purified from chloroplasts (Caffarri et al., 2001). Next, absorbance of these components was measured in the range 360 to 800 nm using a Cary 4000 spectrophotometer. Additionally, the absorbance spectrum of the PSII $C_2S_2M_2$ supercomplex (dimeric core complex with two strongly and two moderately bound LHCII trimers and two sets of minor antenna: CP24, CP26, and CP29) of *Arabidopsis thaliana* (Caffarri et al., 2009) was used. We did not have sufficient material to purify this complex from our plants; however, the absorbance spectra of LHCII and PSI purified from our cucumber or from *Arabidopsis* did not show relevant differences (see Supplemental Figure 6 online). Consequently, no significant differences between $C_2S_2M_2$ in *Arabidopsis* and our leaves are expected. The relative absorbance spectrum of the two photosystems was calculated as follows. First, the LHCII, $C_2S_2M_2$, and PSI-LHCI spectra where normalized in the Q_y region (630 to 750 nm), taking into account the number of coordinated chlorophylls *a* and *b* (Table 2) and the 0.7 times weaker oscillator strengths for chlorophyll *b* compared with chlorophyll *a* in this

region (Sauer et al., 1966). Second, the absorbance spectra of both PSII and PSI were calculated taking into account the LHCII:PSII core and PSI:PSII ratio (see Supplemental Figure 4 online). Third, the ratio between the two spectra was determined as (absorbance PSII)/(absorbance PSI + absorbance PSII) for each light spectrum treatment. This calculation assumes that in vitro all LHCII remained associated with PSII and therefore takes no account of state transitions.

Statistics

Fisher's LSD was used to make post-hoc multiple comparisons among growth light treatment means for pigment and photosystem composition from significant one-way analysis of variance tests ($P < 0.05$) using Genstat (release 9.2; Rothamsted Experimental Station). Likewise, comparisons among the means of growth light spectrum, measuring light spectrum, and the interaction between these two factors were made from significant two-way analysis of variance tests ($P < 0.05$) for the wavelength dependence of the quantum yield for CO_2 fixation, Φ_{PSI}, and Φ_{PSII} and the wavelength dependence of F_0'/F_0.

Supplemental Data

The following materials are available in the online version of this article.

Supplemental Figure 1. Typical Responses of Net Assimilation to Light-Limited Irradiance for Leaves Grown under the Different Light Spectra.

Supplemental Figure 2. Analysis of LHCII Content in Thylakoids of Leaves Grown under a Sunlight Spectrum, a Shade Light Spectrum, and Blue Light.

Supplemental Figure 3. Quantification of PSI/PSII Ratio by Protein Immunoblotting.

Supplemental Figure 4. Absorbance Spectra of LHCII and PSI-LHCI Purified from Chloroplasts of Cucumber Leaves and That of the PSII $C_2S_2M_2$ Supercomplex of *Arabidopsis*.

Supplemental Figure 5. Relationship between the Excitation Balance of the Two Photosystems Using an in Vitro and in Vivo Approach.

Supplemental Figure 6. Absorbance Spectra of the Purified LHCII Trimer and PSI-LHCI of Cucumber Leaves and *Arabidopsis*.

Supplemental Table 1. The Wavelength Dependence of the Absolute and Relative Quantum Yield for CO_2 Fixation on an Incident Light Basis (Action Spectrum).

Supplemental Table 2. The Wavelength Dependence of the Absolute and Relative Quantum Yield for CO_2 Fixation on an Absorbed Light Basis.

ACKNOWLEDGMENTS

This research is supported by the Dutch Technology Foundation Stichting Technische Wetenschappen (i.e., the applied science division of the Nederlandse Organisatie voor Wetenschappelijk Onderzoek and the Technology Program of the Ministry of Economic Affairs), Philips, Plant Dynamics, the Dutch Ministry of Economic Affairs, Agriculture and Innovation, and Productschap Tuinbouw. The work in Amsterdam was supported by NWO (Earth and Life Sciences) via a Vici grant. We thank Joost Ruijsch, Evert Janssen, Rob van der Schoor, and Henk Jalink for their technical support and Jan Snel for his contribution to the light sources. We also thank Frank Millenaar (de Ruiter Seeds) for supplying albino cucumber seeds, Ep Heuvelink for advice on statistics, and Olaf van Kooten and Izabela Witkowska for critical reading of the article.

AUTHOR CONTRIBUTIONS

S.W.H., R.C., E.W., and J.H. designed the research. S.W.H., E.W., and P.D. performed research. S.W.H., E.W., W.v.I., R.C., and J.H. contributed new analytic/computational tools. S.W.H., E.W., P.D., and G.T. analyzed data. S.W.H., R.C., E.W., and J.H. wrote the article.

Received March 18, 2012; revised April 23, 2012; accepted April 30, 2012; published May 22, 2012.

REFERENCES

Ahmad, M., Grancher, N., Heil, M., Black, R.C., Giovani, B., Galland, P., and Lardemer, D. (2002). Action spectrum for cryptochrome-dependent hypocotyl growth inhibition in Arabidopsis. Plant Physiol. **129:** 774–785.

Allen, J.F. (1992). Protein phosphorylation in regulation of photosynthesis. Biochim. Biophys. Acta **1098:** 275–335.

Andrews, J.R., Bredenkamp, G.J., and Baker, N.R. (1993). Evaluation of the role of state transitions in determining the efficiency of light utilization for CO_2 assimilation in leaves. Photosynth. Res. **38:** 15–26.

Bailey, S., Walters, R.G., Jansson, S., and Horton, P. (2001). Acclimation of *Arabidopsis thaliana* to the light environment: The existence of separate low light and high light responses. Planta **213:** 794–801.

Baker, N.R. (2008). Chlorophyll fluorescence: A probe of photosynthesis *in vivo*. Annu. Rev. Plant Biol. **59:** 89–113.

Baker, N.R., Harbinson, J., and Kramer, D.M. (2007). Determining the limitations and regulation of photosynthetic energy transduction in leaves. Plant Cell Environ. **30:** 1107–1125.

Ballottari, M., Dall'Osto, L., Morosinotto, T., and Bassi, R. (2007). Contrasting behavior of higher plant photosystem I and II antenna systems during acclimation. J. Biol. Chem. **282:** 8947–8958.

Bassi, R., Giacometti, G.M., and Simpson, D.J. (1988). Changes in the organization of stroma membranes induced by *in vivo* state-1-state 2 transition. Biochim. Biophys. Acta **935:** 152–165.

Björkman, O., and Demmig, B. (1987). Photon yield of O2 evolution and chlorophyll fluorescence characteristics at 77 K among vascular plants of diverse origins. Planta **170:** 489–504.

Bräutigam, K. et al. (2009). Dynamic plastid redox signals integrate gene expression and metabolism to induce distinct metabolic states in photosynthetic acclimation in *Arabidopsis*. Plant Cell **21:** 2715–2732.

Broess, K., Trinkunas, G., van Hoek, A., Croce, R., and van Amerongen, H. (2008). Determination of the excitation migration time in photosystem II consequences for the membrane organization and charge separation parameters. Biochim. Biophys. Acta **1777:** 404–409.

Caffarri, S., Croce, R., Breton, J., and Bassi, R. (2001). The major antenna complex of photosystem II has a xanthophyll binding site not involved in light harvesting. J. Biol. Chem. **276:** 35924–35933.

Caffarri, S., Kouril, R., Kereïche, S., Boekema, E.J., and Croce, R. (2009). Functional architecture of higher plant photosystem II supercomplexes. EMBO J. **28:** 3052–3063.

Caffarri, S., Passarini, F., Bassi, R., and Croce, R. (2007). A specific binding site for neoxanthin in the monomeric antenna proteins CP26 and CP29 of photosystem II. FEBS Lett. **581:** 4704–4710.

Chow, W.S., Melis, A., and Anderson, J.M. (1990). Adjustments of photosystem stoichiometry in chloroplasts improve the quantum efficiency of photosynthesis. Proc. Natl. Acad. Sci. USA **87:** 7502–7506.

Croce, R., Canino, G., Ros, F., and Bassi, R. (2002). Chromophore organization in the higher-plant photosystem II antenna protein CP26. Biochemistry **41:** 7334–7343.

Croce, R., Müller, M.G., Bassi, R., and Holzwarth, A.R. (2001). Carotenoid-to-chlorophyll energy transfer in recombinant major light-harvesting complex (LHCII) of higher plants. I. Femtosecond transient absorption measurements. Biophys. J. **80:** 901–915.

de Weerd, F.L., Dekker, J.P., and van Grondelle, R. (2003a). Dynamics of β-carotene-to-chlorophyll singlet energy transfer in the core of photosystem II. J. Phys. Chem. B **107:** 6214–6220.

de Weerd, F.L., Kennis, J.T.M., Dekker, J.P., and van Grondelle, R. (2003b). β-Carotene to chlorophyll singlet energy transfer in the photosystem I core of *Synechococcus elongatus* proceeds via the β-carotene S_2 and S_1 states. J. Phys. Chem. B **107:** 5995–6002.

Dietzel, L., Bräutigam, K., and Pfannschmidt, T. (2008). Photosynthetic acclimation: State transitions and adjustment of photosystem stoichiometry—functional relationships between short-term and long-term light quality acclimation in plants. FEBS J. **275:** 1080–1088.

Eichelmann, H., and Laisk, A. (2000). Cooperation of photosystems II and I in leaves as analyzed by simultaneous measurements of chlorophyll fluorescence and transmittance at 800 nm. Plant Cell Physiol. **41:** 138–147.

Emerson, R., Chalmers, R., and Cederstrand, C. (1957). Some factors influencing the long-wave limit of photosynthesis. Proc. Natl. Acad. Sci. USA **43:** 133–143.

Evans, J.R. (1986). A quantitative analysis of light distribution between the two photosystems, considering variation in both the relative amounts of the chlorophyll-protein complexes and the spectral quality of light. Photobiochem. Photobiophys. **10:** 135–147.

Evans, J.R. (1987). The dependence of quantum yield on wavelength and growth irradiance. Aust. J. Plant Physiol. **14:** 69–79.

Evans, J.R., and Anderson, J.M. (1987). Absolute absorption and relative fluorescence excitation spectra of the 5 major chlorophyll-protein complexes from spinach thylakoid membranes. Biochim. Biophys. Acta **892:** 75–82.

Fey, V., Wagner, R., Braütigam, K., Wirtz, M., Hell, R., Dietzmann, A., Leister, D., Oelmüller, R., and Pfannschmidt, T. (2005). Retrograde plastid redox signals in the expression of nuclear genes for chloroplast proteins of *Arabidopsis thaliana*. J. Biol. Chem. **280:** 5318–5328.

Fujita, Y. (1997). A study on the dynamic features of photosystem stoichiometry: Accomplishments and problems for future studies. Photosynth. Res. **53:** 83–93.

Genty, B., Briantais, J.M., and Baker, N.R. (1989). The relationship between the quantum yield of photosynthetic electron transport and quenching of chlorophyll fluorescence. Biochim. Biophys. Acta **990:** 87–92.

Gitelson, A.A., Zur, Y., Chivkunova, O.B., and Merzlyak, M.N. (2002). Assessing carotenoid content in plant leaves with reflectance spectroscopy. Photochem. Photobiol. **75:** 272–281.

Govindjee (1999). On the requirement of minimum number of four versus eight quanta of light for the evolution of one molecule of oxygen in photosynthesis: A historical note. Photosynth. Res. **59:** 249–254.

Haldrup, A., Jensen, P.E., Lunde, C., and Scheller, H.V. (2001). Balance of power: A view of the mechanism of photosynthetic state transitions. Trends Plant Sci. **6:** 301–305.

Hogewoning, S.W., Douwstra, P., Trouwborst, G., van Ieperen, W., and Harbinson, J. (2010b). An artificial solar spectrum substantially alters plant development compared with usual climate room irradiance spectra. J. Exp. Bot. **61:** 1267–1276.

Hogewoning, S.W., and Harbinson, J. (2007). Insights on the development, kinetics, and variation of photoinhibition using chlorophyll fluorescence imaging of a chilled, variegated leaf. J. Exp. Bot. **58:** 453–463.

Hogewoning, S.W., Trouwborst, G., Harbinson, J., and van Ieperen, W. (2010a). Light distribution in leaf chambers and its consequences for photosynthesis measurements. Photosynthetica **48:** 219–226.

Hogewoning, S.W., Trouwborst, G., Maljaars, H., Poorter, H., van Ieperen, W., and Harbinson, J. (2010c). Blue light dose-responses of leaf photosynthesis, morphology, and chemical composition of *Cucumis sativus* grown under different combinations of red and blue light. J. Exp. Bot. **61:** 3107–3117.

Hoover, W.H. (1937). The dependence of carbon dioxide assimilation in a higher plant on wavelength of radiation. Smithsonian Institution Misc. Collections **95:** 1–13.

Inada, K. (1976). Action spectra for photosynthesis in higher plants. Plant Cell Physiol. **17:** 355–365.

Jackson, J.A., and Jenkins, G.I. (1995). Extension-growth responses and expression of flavonoid biosynthesis genes in the *Arabidopsis hy4* mutant. Planta **197:** 233–239.

Jarillo, J.A., Gabrys, H., Capel, J., Alonso, J.M., Ecker, J.R., and Cashmore, A.R. (2001). Phototropin-related NPL1 controls chloroplast relocation induced by blue light. Nature **410:** 952–954.

Kingston-Smith, A.H., Harbinson, J., and Foyer, C.H. (1999). Acclimation of photosynthesis, H_2O_2 content and antioxidants in maize (*Zea mays*) grown at sub-optimal temperatures. Plant Cell Environ. **22:** 1071–1083.

Kramer, D.M., Johnson, G., Kiirats, O., and Edwards, G.E. (2004). New fluorescence parameters for the determination of Q_A redox state and excitation energy fluxes. Photosynth. Res. **79:** 209–218.

Kubasek, W.L., Shirley, B.W., McKillop, A., Goodman, H.M., Briggs, W., and Ausubel, F.M. (1992). Regulation of flavonoid biosynthetic genes in germinating *Arabidopsis* seedlings. Plant Cell **4:** 1229–1236.

Long, S.P., Postl, W.F., and Bolharnordenkampf, H.R. (1993). Quantum yields for uptake of carbon dioxide in C_3 vascular plants of contrasting habitats and taxonomic groupings. Planta **189:** 226–234.

McCree, K.J. (1972a). Significance of enhancement for calculations based on the action spectrum for photosynthesis. Plant Physiol. **49:** 704–706.

McCree, K.J. (1972b). Action spectrum, absorptance and quantum yield of photosynthesis in crop plants. Agric. Meteorol. **9:** 191–216.

Melis, A. (1991). Dynamics of photosynthetic membrane composition and function. Biochim. Biophys. Acta **1058:** 87–106.

Melis, A., Murakami, A., Nemson, J.A., Aizawa, K., Ohki, K., and Fujita, Y. (1996). Chromatic regulation in *Chlamydomonas reinhardtii* alters photosystem stoichiometry and improves the quantum efficiency of photosynthesis. Photosynth. Res. **47:** 253–265.

Morosinotto, T., Bassi, R., Frigerio, S., Finazzi, G., Morris, E., and Barber, J. (2006). Biochemical and structural analyses of a higher plant photosystem II supercomplex of a photosystem I-less mutant of barley. Consequences of a chronic over-reduction of the plastoquinone pool. FEBS J. **273:** 4616–4630.

Oxborough, K., and Baker, N.R. (1997). Resolving chlorophyll *a* fluorescence images of photosynthetic efficiency into photochemical and non-photochemical components - calculation of *qP* and *Fv'/Fm'* without measuring *Fo'*. Photosynth. Res. **54:** 135–142.

Pfannschmidt, T. (2005). Acclimation to varying light qualities: Toward the functional relationship of state transitions and adjustment of photosystem stoichiometry. J. Phycol. **41:** 723–725.

Pospísil, P. (2009). Production of reactive oxygen species by photosystem II. Biochim. Biophys. Acta **1787:** 1151–1160.

Quigg, A., Kevekordes, K., Raven, J.A., and Beardall, J. (2006). Limitations on microalgal growth at very low photon fluence rates: The role of energy slippage. Photosynth. Res. **88:** 299–310.

Sager, J.C., Smith, W.O., Edwards, J.L., and Cyr, K.L. (1988). Photosynthetic efficiency and phytochrome photoequilibria determination using spectral data. Trans. ASAE **31:** 1882–1889.

Samson, G., and Bruce, D. (1995). Complementary changes in absorption cross-sections of photosystems I and II due to phosphorylation and

Mg^{2+}-depletion in spinach thylakoids. Biochim. Biophys. Acta **1232:** 21–26.

Sauer, K., Lindsay Smith, J.R., and Schultz, A.J. (1966). Dimerization of chlorophyll a, chlorophyll b, and bacteriochlorophyll in solution. J. Am. Chem. Soc. **88:** 2681–2688.

Schägger, H. (2006). Tricine-SDS-PAGE. Nat. Protoc. **1:** 16–22.

Sharp, R.E., Matthews, M.A., and Boyer, J.S. (1984). Kok effect and the quantum yield of photosynthesis: Light partially inhibits dark respiration. Plant Physiol. **75:** 95–101.

Solfanelli, C., Poggi, A., Loreti, E., Alpi, A., and Perata, P. (2006). Sucrose-specific induction of the anthocyanin biosynthetic pathway in Arabidopsis. Plant Physiol. **140:** 637–646.

Sonneveld, P.J., Swinkels, G.L.A.M., and Bot, G.P.A. (2009). Design of a solar greenhouse with energy delivery by the conversion of near infrared radiation - Part 1 optics and PV-cells. Acta Hortic. **807:** 47–54.

Terashima, I., Fujita, T., Inoue, T., Chow, W.S., and Oguchi, R. (2009). Green light drives leaf photosynthesis more efficiently than red light in strong white light: Revisiting the enigmatic question of why leaves are green. Plant Cell Physiol. **50:** 684–697.

van Kooten, O., and Snel, J.F.H. (1990). The use of chlorophyll fluorescence nomenclature in plant stress physiology. Photosynth. Res. **25:** 147–150.

von Caemmerer, S., and Farquhar, G.D. (1981). Some relationships between the biochemistry of photosynthesis and the gas exchange of leaves. Planta **153:** 376–387.

Walters, R.G., and Horton, P. (1994). Acclimation of *Arabidopsis thaliana* to the light environment: Changes in composition of the photosynthetic apparatus. Planta **195:** 248–256.

Walters, R.G., and Horton, P. (1995). Acclimation of *Arabidopsis thaliana* to the light environment: Changes in photosynthetic function. Planta **197:** 306–312.

Walters, R.G., Rogers, J.J.M., Shephard, F., and Horton, P. (1999). Acclimation of *Arabidopsis thaliana* to the light environment: The role of photoreceptors. Planta **209:** 517–527.

Wientjes, E., van Stokkum, I.H.M., van Amerongen, H., and Croce, R. (2011). The role of the individual Lhcas in photosystem I excitation energy trapping. Biophys. J. **101:** 745–754.

Yakushevska, A.E., Jensen, P.E., Keegstra, W., van Roon, H., Scheller, H.V., Boekema, E.J., and Dekker, J.P. (2001). Supermolecular organization of photosystem II and its associated light-harvesting antenna in *Arabidopsis thaliana*. Eur. J. Biochem. **268:** 6020–6028.

Yamamoto, Y., Aminaka, R., Yoshioka, M., Khatoon, M., Komayama, K., Takenaka, D., Yamashita, A., Nijo, N., Inagawa, K., Morita, N., Sasaki, T., and Yamamoto, Y. (2008). Quality control of photosystem II: Impact of light and heat stresses. Photosynth. Res. **98:** 589–608.

Zheng, S.-J., Snoeren, T.A.L., Hogewoning, S.W., van Loon, J.J.A., and Dicke, M. (2010). Disruption of plant carotenoid biosynthesis through virus-induced gene silencing affects oviposition behaviour of the butterfly *Pieris rapae*. New Phytol. **186:** 733–745.